JACS
JOURNAL OF THE AMERICAN CHEMICAL SOCIETY

ARTICLE

pubs.acs.org/JACS

Reversible Phase Transitions within Self-Assembled Fibrillar Networks of (*R*)-18-(*n*-Alkylamino)octadecan-7-ols in Their Carbon Tetrachloride Gels

V. Ajay Mallia,[†] Paul D. Butler,[‡] Bijay Sarkar,[†] K. Travis Holman,[†] and Richard G. Weiss*[,†]

[†]Department of Chemistry, Georgetown University, Washington, D.C. 20057-1227, United States

[‡]NIST Center for Neutron Research, National Institute of Standards and Technology, Gaithersburg, Maryland 20899-8562, United States

Supporting Information

ABSTRACT: The CCl_4 gel phases of a series of low-molecular-mass organogelators, (*R*)-18-(*n*-alkylamino)octadecan-7-ols (**HSN-*n***, where $n = 0-5, 18$ is the alkyl chain length), appear to be unprecedented in that the fibrillar networks of some of the homologues undergo thermally reversible, gel-to-gel phase transitions, and some of those transitions are evident as opaque−transparent changes in the appearance of the samples. The gels have been examined at different concentrations and temperatures by a wide variety of spectroscopic, diffraction, thermal, and rheological techniques. Analyses of those data and data from the neat gelators have led to an understanding of the source of the gel-to-gel transitions. IR and SANS data implicate the expulsion (on heating the lower-temperature gel) or the inclusion (on cooling the higher-temperature gel) of molecules of CCl_4 that are interspersed between fibers in bundles. However, the root cause of the transitions is a consequence of changes in the molecular packing of the **HSN-*n*** within the fibers. This study offers opportunities to design new gelators that are capable of behaving in multiple fashions without entering the sol/solution phase, and it identifies a heretofore unknown transformation of organogels.

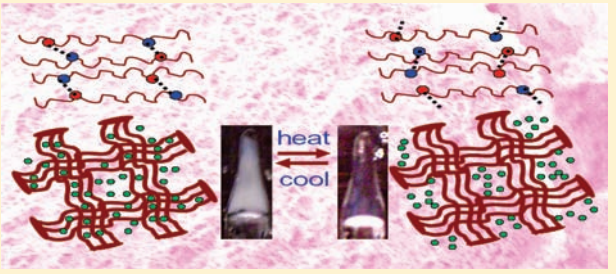

INTRODUCTION

Organogels are thermally reversible quasi-solid materials composed of an organic liquid (in the present work, CCl_4) and low concentrations of low-molecular-mass molecules (gelators, LMOGs).[1] The LMOGs self-assemble to form fibrillar networks (SAFINs) via weak physical interactions (van der Waals forces, intermolecular H-bonding, electrostatic forces, $\pi-\pi$ stacking, or London dispersion forces), predominantly by one-dimensional growth modes.[2] The process of gelation is a fine balance of molecules that self-assemble in solvents, depending on the gelator−gelator and gelator−solvent interactions.[3] Some polymer gels (i.e., cross-linked polymers swollen with liquid)[4] and LMOG gels with liquid crystals as the liquid component[5] are known to undergo temperature-induced, gel-to-gel transitions. However, we are aware of only one report in which an LMOG has been shown to undergo a thermally induced phase transition within its SAFIN.[6] In that case, the gelator was a known discotic liquid crystal, and the phase transitions found in the bulk and in the fibrillar networks of its gels were similar in nature but occurred at different temperatures.

Many LMOGs are known to be polymorphic—that is, more than one molecular packing arrangement can be identified, depending on the details of their heating or cooling protocols when neat or when forming fibrillar networks in gels from different solvents.[7−9] Here, we report that a class of non-liquid-crystalline gelators, (*R*)-18-(*n*-alkylamino)octadecan-7-ols (**HSN-*n***), undergo first-order gel-to-gel phase transitions, leading apparently to different morphs, in their carbon tetrachloride gels.

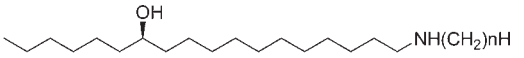

HSN-n (**n** = 0-5,18)

The transitions were first noted as a curiosity, and not investigated, in our recent studies with these gelators.[10] On closer scrutiny, they became a fascinating puzzle that includes unprecedented transformations within fibrillar networks of organogels. The transitions are not related to temperature-induced changes in the CCl_4 liquid and, at least in some of the **HSN-*n*** (see especially $n = 3$), are not observed in the neat solids. Also, CCl_4 is the *only* liquid (of several tested)[10] which leads to gels that exhibit the transitions! Analyses of the rheological, thermal, and structural properties of the gels, in both their lower- and higher-temperature gel phases, provide insights into the origin and nature of the transitions. To the best of our knowledge, this form of gel-to-gel phase transition is unprecedented, and it opens the

Received: May 12, 2011
Published: July 06, 2011

dx.doi.org/10.1021/ja204371b | *J. Am. Chem. Soc.* 2011, 133, 15045–15054

possibility to design molecular gels with a new dimension of versatility and potential applications. A very remotely related phenomenon, a temperature-induced phase transition of poly(*N*-isopropylacrylamide) hydrogels, is attributed to conformational changes—folding and unfolding of the polymer chains—as water molecules near them are expelled or added.[11,12] As will be shown, the gel-to-gel transformations of the **HSN-*n*** are based upon a completely different process: a change of the molecular packing arrangement within the fibers constituting the gel networks. Moreover, the enormous sensitivity of the structures of the **HSN-*n*** as gelators of CCl_4 and the types of SAFINs that they produce [N.B., the addition or subtraction of one $-(CH_2)-$ group along the *N*-alkyl chain] demonstrate that the energetics associated with the aggregation and one-dimensional assembly of these molecules is a delicate balance of several factors.

EXPERIMENTAL SECTION

Materials. (*R*)-18-Aminooctadecan-7-ol (**HSN-0**) and the (*R*)-18-(alkylamino)octadecan-7-ols (**HSN-*n***, with $n = 1-5$ and 18) were prepared as described previously.[10] CCl_4 (reagent grade, Fischer Scientific) was used as received.

Methods. "Fast-cooled" gels were prepared by heating a mixture of the gelator and CCl_4 in a flame-sealed glass tube (~5 mm i.d.) until a solution/sol was obtained and then placing the tube directly into an ice−water bath (~5 °C) for 10 min. Thereafter, the tube was left at 23−24 °C for 1 h, and its appearance was noted. The procedure for preparation of "slow-cooled" gels was the same except that the hot solution/sol was kept in the water bath while it returned slowly to room temperature (~2 °C/min). Unless stated otherwise, all gels were prepared by the fast-cooling protocol. Gelation temperatures (T_{gs}) were determined by the falling drop method[13] as the temperature range over which the gels (in the inverted tubes) fell under the influence of gravity when heated at ~1.5 °C/min in a water bath. The critical gelator concentrations (CGCs) are the lowest concentrations of the **HSN-*n*** in CCl_4 that did not fall when a sample tube was inverted at 24 °C.

Polarizing optical microscopy (POM) images were recorded on a Leitz 585 SM-LUX-POL optical microscope equipped with crossed polars, a Leitz 350 heating stage, and a CCD camera (Photometrics Coolsnap) interfaced to a computer, and the image was viewed using RS image (version1.9.2) software. Sample temperatures (corrected) were measured using a microprocessor (Omega HH503) connected to a K (Chrome-Alome) thermocouple (Omega Engineering Inc.). The gel samples were flame-sealed in flattened glass capillary tubes (0.4 mm path-length, VitroCom, NJ), heated to their sol phases, and cooled according to the protocols described below. Differential scanning calorimetry (DSC) measurements at heating and cooling rates of 10 °C/min were carried out on a Q200 calorimeter (TA Instruments) interfaced to a TA Thermal Analyst 3100 controller that was connected to an RCS90 cooling system under a stream of nitrogen (50 mL/min). Gel samples for DSC were placed in hermetically sealed Tzero lids and pans. In none of the experiments reported was any weight loss detected after the DSC runs.

Powder X-ray diffraction (XRD) studies were performed on a Rigaku R-AXIS image plate system diffractometer with Cu Kα X-rays ($\lambda = 1.54$ Å, 46 kV, and 40 mA). Data processing and analyses employed Rigaku Rapid Control software (version 2.3.3) and Rigaku area Max2 (Version 2 RC2 2005), respectively, and indexing was performed using Materials Data JADE (version 5.0.35) software. Gel samples were sealed in 0.5 mm glass capillaries, and neat **HSN-*n*** were sealed in 1 mm glass capillaries (both from W. Müller, Schönwalde, Germany). Diffraction data were collected for 90 min for the neat gelators and 10 h for the gel samples and neat CCl_4.

The packing structure of a 0.75 × 0.44 × 0.10 mm single crystal of (*R*)-18-(pentylamino)octadecan-7-ol (**HSN-5**), prepared by slow evaporation of a 1:3 acetone:methanol solution, was solved by X-ray diffraction on a Siemens SMART 1000 CCD platform diffractometer equipped with an APEX II CCD detector (Bruker-AXS) with graphite-monochromated Mo Kα radiation ($\lambda = 0.71$ Å) at −173 °C. Experimental parameters for analysis are collected in Supporting Information Table S1. All non-hydrogen atoms were modeled with anisotropic displacement parameters. All hydrogen atoms were placed in calculated positions and refined using a riding model with coordinates and isotropic displacement parameters being dependent upon the atom to which they are attached. The amine hydrogen atom could not be located in the difference Fourier map and was not included in the model. The unit cell was determined from 8483 reflections in the range of $1.27° < \theta < 28.0°$. The data were integrated using the SAINT software. The structure was solved by direct methods and refined iteratively via full-matrix least-squares and difference Fourier analysis using the SHELX-97 software[14] and with the assistance of X-SEED.[15]

Scanning electron microscopy (SEM) images were recorded on a Zeiss SEM (Supra 55 VP, 2−30 kV) on samples prepared by placing a small drop of gel on an Al mount (1/200 slotted head, 1/800 pin, Ted Pella, Inc.) and allowing the liquid to evaporate at 24 °C for 24 h. No metal coating was applied. Cryo-SEM imaging of the gel was performed on a cold field-emission SEM (Hitachi S-4800). The sample preparation procedure for the CCl_4 gel involved rapid plunging of the sample into slushed liquid nitrogen, followed by freeze-fracture using the flat edge of a cold (−130 °C) knife. The sample was then sputter-coated with gold−palladium at 10 mA for 88 s and imaged on the SEM at a voltage of 1 kV in TV image mode.

IR studies were carried out on a Nicolet 380 FT-IR spectrometer using liquid cells having NaCl windows and sealed with Teflon plugs. Superambient temperatures were attained by wrapping the cell, except for the windows, with resistors connected to a filament transformer (100 V (in), 6 V (out), 6 A) and a Variac variable autotransformer. Sample temperatures (corrected) were measured using an Omega HH503 microprocessor connected to a K thermocouple which was placed on the aluminum block holding the NaCl windows. Relative turbidity measurements were made using a Cary 300 BIO UV−vis spectrophotometer. The gel samples were prepared using a fast-cooling protocol and flame-sealed in flattened glass capillary tubes (0.4 mm path length, VitroCom, NJ). Temperature was maintained by a thermostated, circulating bath.

Rheological measurements were obtained on a strain-controlled rheometer (Anton Paar Physica MCR 301) using 25 mm diameter parallel plates and a Peltier heater/cooler system. The data were collected using Rheoplus/32 Service V3.10 software (Anton Paar). Gel aliquots were quickly loaded onto the bottom plate at ~22 °C, compressed to a 0.5 mm gap with the upper plate, and cooled to 15 °C. To minimize liquid evaporation, the rheometer sample compartment was covered with a solvent trap in which thin layers of CCl_4-soaked paper were placed.

Small-angle neutron scattering (SANS) measurements were performed at the NIST Center for Neutron Research (NCNR) using the NG7 SANS instrument.[16] The scattering intensities were corrected for background noise, detector efficiency, empty cell scattering, and sample transmission and were placed on an absolute scale using beam flux measurements with the NCNR-supplied IGOR software tools.[17] Ultra-small-angle neutron scattering (USANS) measurements were also performed at the NCNR using the thermal neutron double-crystal diffractometer (BT5) and corrected in the usual way.[18] The Q ranges ($Q = 4\pi/\lambda \sin(\theta)/2$ is the momentum transfer vector and is inversely proportional to the length scales probed) of the SANS and USANS overlap around $Q = 0.001$ Å^{-1}. However, the USANS uses an infinite slit source so that the resolution effects compared to the pinhole SANS are

massive. The USANS slit-smeared intensities were numerically desmeared using the IGOR software tools[18] in order to plot the intensity over the entire Q range (SANS + USANS). The excellent agreement between the de-smeared USANS and SANS demonstrates the accuracy of the corrections to absolute scale as well as of the de-smearing algorithm. Samples were prepared in 1 mm path length cells with Suprasil quartz windows and stainless steel bodies. The samples were then cycled several times through the gel-to-gel transition to verify accessibility and reproducibility of the two gel states in the cell and to verify the integrity of the sample and cell throughout the temperature-cycling process.

RESULTS AND DISCUSSION

During the study of the organogels of the amide and amine derivatives of (*R*)-12-hydroxyoctadecanoic acid (**HSA**),[10] a well-known and efficient LMOG,[19] an unanticipated opaque-to-clear phase transition that did not involve the formation of a sol was observed in a **HSN-3**/CCl_4 gel. Examination by DSC revealed an endotherm on heating and an exotherm on cooling at nearly the same temperatures, but no phase transition could be detected when the neat **HSN-3** was heated and cooled over a wide temperature range, <0 to >100 °C. Those observations led to a detailed systematic investigation of the curious transition. Although similar transitions were observed in CCl_4 gels of some of the other **HSN-*n*** examined, none was found for **HSN-*n*** gels in which a different liquid was employed!

Molecular Packing of Neat Gelators. Although there are relatively few diffraction lines in the XRD curves of the **HSN-*n*** powders, they are consistent with monoclinic packing arrangements (Supporting Information Tables S2 and S3 and Figures S1−S4). Only **HSN-1** and one of the morphs of 18-(ethylamino)octadecan-7-ol (**HSN-2**, vide infra) has a unit cell β angle that differs from 95°. From the single-crystal structure determination, molecules of 18-(pentylamino)octadecan-7-ol (**HSN-5**) are arranged in a head-to-tail arrangement, with the amine-NH of one molecule hydrogen-bonded to the hydroxyl group of a neighbor (Figure 1I). The net result is a one-dimensional network of hydrogen bonds nearly perpendicular to the extended long axes of the molecules. Gelator networks self-assemble usually by one-dimensional growth modes[2] to form fibers, strands, or tapes via relatively weak physical molecular interactions.

Comparisons of the powder diffractogram of **HSN-5** constructed from the single-crystal XRD data at −173 °C and that of powdered **HSN-5** at 22 °C (Supporting Information Figure S5) show small shifts in the wider-angle reflections due to the thermal expansion of the unit cell at the higher temperature,[20] but the diffractograms are otherwise the same. Thus, there was no solid−solid phase transition between −173 and 22 °C. DSC thermograms showed no solid−solid phase transitions in 18-(alkylamino)-octadecan-7-ols on heating or cooling, at least within the temperature ranges examined, from <0 to >100 °C (Supporting Information Figures S6−S10 and Table S4).

The IR spectrum of neat **HSN-5** includes a sharp peak at 3270 cm^{-1} and a broad band at 3120 cm^{-1} (Figure 1II, e) that can be assigned to NH- and OH-stretching modes, respectively, of bonds that are involved in strong H-bonding interactions. Such interactions are expected on the basis of the crystal structure shown in Figure 1I. Normally, the hydrogen-bonded OH-stretching peak is observed around 3200 cm^{-1}. The ~80 cm^{-1} red-shift from 3200 cm^{-1} observed in the hydrogen

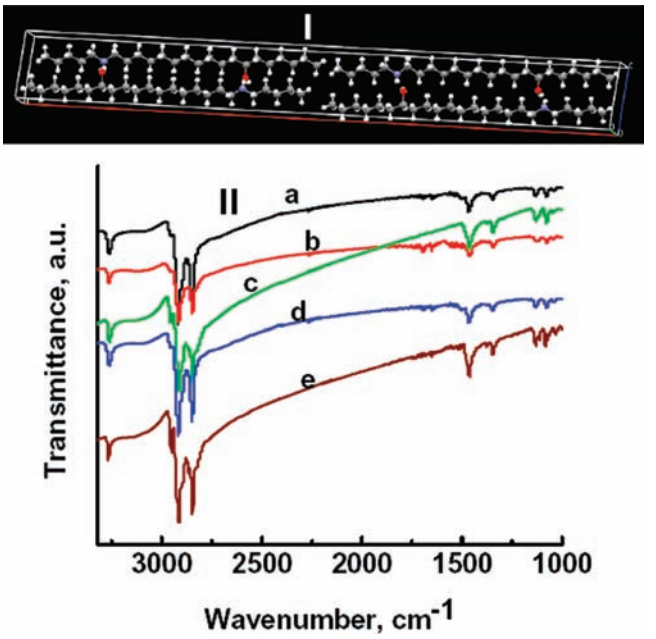

Figure 1. (I) X-ray crystal structure of (*R*)-18-(pentylamino)-octadecan-7-ol (**HSN-5**). (II) IR spectra of neat (a) **HSN-1**, (b) **HSN-2**, (c) **HSN-3**, (d) **HSN-4**, and (e) **HSN-5**.

bonded OH-stretching peak of **HSN-5** is consistent with the strong hydrogen-bonding interaction between OH and secondary amine groups.[21] A similar red-shift in the OH-stretching peak has been reported for the IR spectrum of a mixture of phenol and diethyl amine.[21] Because the IR spectra of the other neat **HSN-*n*** display virtually the same frequencies and peak shapes as **HSN-5**, we conclude that the crystalline packing of this group of **HSN-*n*** is in a head-to-tail arrangement, like (but not necessarily the same as) that shown in Figure 1I.

The neat solid of 18-(ethylamino)octadecan-7-ol (**HSN-2**) from evaporation of a 1:4 (v:v) ethyl acetate:hexane solution is a mixture of two crystal morphs. Unfortunately, it was not possible to separate the morphs physically and examine them alone, and attempts to isolate one of the crystal forms from different solvent mixtures were unsuccessful. Both morphs could be indexed[22] as monoclinic, one of which is similar to that for **HSN-5** (Supporting Information Figure S2 and Table S2). The similarities between the IR spectra of **HSN-2** and **HSN-5** strengthen the monoclinic assignment of one of the **HSN-2** morphs. However, DSC thermograms of **HSN-2** showed no evidence of two separate melting endotherms (Supporting Information Figure S7); the melting temperatures must be very similar, or the heat of the morph−morph transition (if they interconvert) must be very low.

Gel-to-Gel Phase Transitions in CCl_4. The phase behavior of ~2 wt % **HSN-*n*** in CCl_4 is summarized in Table 1. The primary amine **HSN-0** and *N*-octadecyl derivative **HSN-18** did not gelate CCl_4 and, therefore, will not be discussed here in detail. Within specific concentration ranges in carbon tetrachloride, gels of 18-(ethylamino)octadecan-7-ol (**HSN-2**) and 18-(propylamino)-octadecan-7-ol (**HSN-3**) exhibited transitions that involved changes in their fibrillar networks but not the overall phase—*these are gel-to-gel transitions*. For example, a 1 wt % **HSN-3**/CCl_4 gel is opaque (OG) below ~30 °C and remains a clear gel (CG) between ~30 and 74−75 °C, the highest temperature examined

Table 1. Appearances,[a] Gel-to-Gel and Gel-to-Sol Transition Temperatures (T_{gg} and T_{gs}, Respectively)[b], and Periods of Stability[c] of Samples Containing ~2 wt % HSN-*n* in CCl_4

HSN-*n*, *n* =	appearance at 24 °C	appearance in higher-temperature gel phase	T_{gg} (°C)	T_{gs} (°C)	stability
0	visc soln				
1	TG			74−75	>6 m
2	OG (syn)	CG	24−30	69−70	>6 m
3	OG	CG	27−32	74−75	>6 m
4	TG	TG	42[d]	72−74	>6 m
5	TG			68	>6 m
18	visc soln				

[a] OG, opaque gel; syn, syneresis; visc soln, viscous solution; TG, translucent gel; CG, clear gel. [b] Detection of T_{gg} by opaque−transparent change and of T_{gs} by the falling drop method. [c] Months (m) between gel preparation in a sealed container and visually detectable phase separation after being kept at ~24 °C. [d] From DSC.

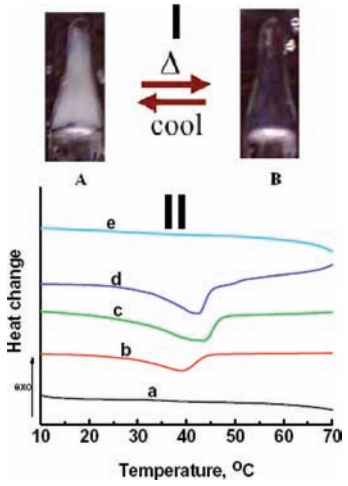

Figure 2. (I) A 1.0 wt % 18-(propylamino)octadecan-7-ol (**HSN-3**)/CCl_4 gel at (A) 20 and (B) 40 °C. (II) DSC thermograms from first heating of ~2 wt % CCl_4 gels of (a) **HSN-1**, (b) **HSN-2**, (c) **HSN-3**, (d) **HSN-4**, and (e) **HSN-5**.

because the boiling point of the CCl_4 liquid is 77 °C. These changes are thermally reversible—the transition is observed visually and by DSC (see, for example, Figure 2) on heating or cooling the gel—and the gel−sol phase transition (detected by the "falling drop" method[13]) is thermally reversible as well. In this case, the gel−sol phase transition could not be detected by DSC (Figure 2II). Gels of 2 wt % **HSN-1**/CCl_4 and **HSN-5**/CCl_4 were translucent and melted to a sol at 74−75 and 68 °C, respectively, without showing an intervening gel-to-gel transition either visually or by DSC (Figure 2 and Supporting Information Figures S11 and S12).

The dependence of the gel-to-gel (T_{gg}) and gel-to-sol (T_{gs}) phase transition temperatures on the concentrations of **HSN-2** and **HSN-3** is shown in Figure 3. Relative turbidity (scattering) at 330 nm from a 2.0 wt % **HSN-3** in CCl_4 gel decreased in intensity on heating at 28 °C and increased slowly upon cooling below this temperature (Supporting Information Figure S13). Both of these

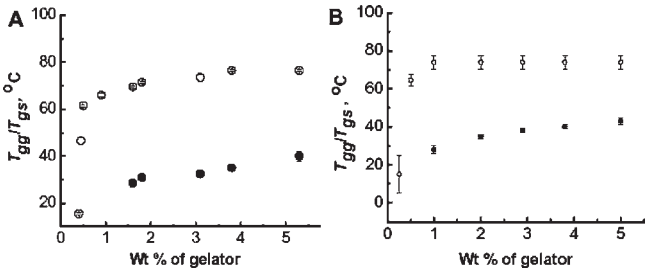

Figure 3. T_{gg} (●) and T_{gs} (○) transition temperatures for CCl_4 gels of (A) **HSN-2** and (B) **HSN-3** as a function of gelator concentration. Vertical bars indicate the temperature ranges where the initial and final portions of an inverted gel sample fell upon slow heating. Note that for the gels for which T_{gs} is near the boiling point of the CCl_4, the gel-to-sol transition may be a result of boiling of the solvent and should not be taken as the "true" T_{gs} value.

observations are consistent with the visual opaque-to-clear gel change in appearance and the hysteresis found in DSC measurements. Scattering at 310 or 330 nm from a 2.1 wt % **HSN-4**/CCl_4 gel did not change perceptibly throughout the entire temperature range examined (Supporting Information Figure S13). As noted, this gel shows a heating endotherm at 42 °C (Figure 2II, d) and a great deal of hysteresis when cooled, but it remains clear to the eye. None of the other 18-(alkylamino)octadecan-7-ol homologues exhibited visual gel-to-gel phase changes in CCl_4 or in any of the other liquids (spanning a wide range of polarities and structures, including liquids that are polychlorinated) that were tested,[10] nor did **HSN-2** and **HSN-3** in any liquid besides CCl_4. Gels with concentrations higher than ~5 wt % gelator were not examined. The T_{gs} values were determined by the falling drop method, and the vertical bars in Figure 3 indicate when the initial and final parts of the sample fell as samples were heated from room temperature at ~1.5 °C/min. T_{gs} values in the "plateau" regions (i.e., where T_{gs} was almost independent of gelator concentration) could not be located by DSC because they seem to be limited by the boiling point of CCl_4. Because no heating endotherms corresponding to the T_{gs} regions were detected by DSC, either the heats involved must be very low or, more likely, the fibrillar networks melt at temperatures that exceed the boiling point of CCl_4. A large portion of the fibrous network may exist above the T_{gs} determined by the falling drop method. Also, gels at very low concentrations (<1 wt %) of **HSN-3** were clear to below room temperature, and they exhibited no visually detectable gel-to-gel transitions even though, for example, the 0.5 wt % gel has a T_{gs} near 60 °C.

From the dependence of T_{gs} for CCl_4 gels on the concentrations of **HSN-1** and **HSN-4** (Supporting Information Figures S14 and S15), the CGC of both LMOGs is <1 wt %, and the plateau value of their T_{gs} is >70 °C at ≥2 wt % concentrations. The *N*-methyl derivative **HSN-1** formed translucent gels in CCl_4 at room temperature that changed to clear sols directly when heated, and DSC thermograms showed no heating endotherms or cooling exotherms corresponding to a gel-to-gel transition (Supporting Information Figure S11), for one or both of the reasons mentioned above.

No visual gel-to-gel transition was detected for translucent gels with 2−5 wt % **HSN-4** in CCl_4 as well, although their POMs consisted of birefringent patterns that changed slightly with temperature below 72−74 °C, the T_{gs} (Supporting Information Figure S16). However, DSC thermograms did provide evidence

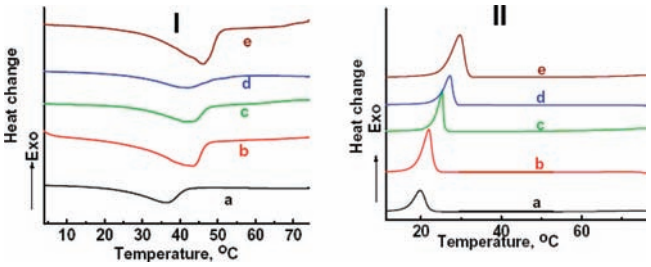

Figure 4. DSC thermograms from first heating of **HSN-3**/CCl_4 gels (I) and first cooling of the corresponding sols (II) as a function of gelator concentration: (a) 1.0, (b) 2.1, (c) 3.1, (d) 4.0, and (e) 4.8 wt %.

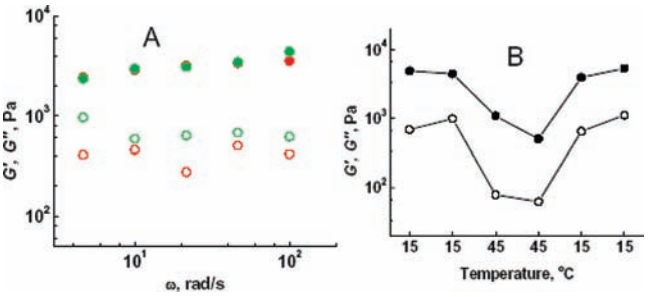

Figure 5. (A) Log−log frequency sweep (0.01% strain) for a 2.1 wt % **HSN-3**/CCl_4 gel at 15 °C, showing data from two runs as red and green symbols. (B) G' (●) and G'' (○) at 0.01% strain and a single frequency (100 rad/s) for a 1.9 wt % **HSN-3**/CCl_4 gel in the sequence of temperatures shown from left to right on the *x*-axis. The time between each 15 and 45 °C run is 30 s, and the time between 15 and 45 °C runs is 4 min. The approximate time for each run is 10 s.

for a gel-to-gel transition. As shown in Supporting Information Figure S17, the 2 wt % gel exhibited a heating endotherm and a cooling exotherm which decreased in both heat and temperature with subsequent heating/cooling cycles. However, the heats and T_{gg} values of the initial heating/cooling cycle were approached slowly when the gel was allowed to stand at ambient temperature for a long period. Thus, the decreases observed upon repeated heating and cooling are a consequence of a hysteresis effect rather than decomposition of **HSN-4**. We conjecture that the slow rate of recovery is related to our inability to heat the sol phases in the hermetically sealed DSC containers to temperatures at which the aggregates are completely dissociated—note, again, our inability to detect gel-to-sol transitions by DSC; the sols retain a memory of their original fibrous networks but cannot reestablish them completely.[23] This behavior is intriguing because a similar lack of complete de-aggregation must be present in the sol phases of **HSN-2** and **HSN-3** as well, yet they display none of the hysteresis of **HSN-4**.

The temperatures at the maximum heat flows (T_m), onsets of endotherms or exotherms (T_t), and enthalpies of transitions for the gel-to-gel transitions of **HSN-3**/CCl_4 gels from DSC thermograms are summarized in Supporting Information Table S6, and the heats normalized to the same concentration of **HSN-3** are presented in Supporting Information Table S7; a large part of the apparent random changes in the normalized enthalpies can be attributed to the broad peak shapes and the imprecision that follows in measuring the peak areas. Figure 4 shows the DSC thermograms (not normalized for total sample weights or for **HSN-3** concentrations) from the first heating and first cooling of CCl_4 gels with different concentrations of **HSN-3**; comparison of the DSC thermograms of these gels formed by slow-cooling reveals that T_{gg} is not sensitive to the cooling protocol (Supporting Information Figure S20), but T_{gg} increases steadily with increasing concentration of **HSN-3**.

Viscoelasticity of Gels. Although they are viscoelastic and able to resist the force of gravity in 5 mm i.d. glass vessels, the **HSN-*n***/CCl_4 gels are weak. For example, it was not possible to prepare large amounts of a **HSN-3**/CCl_4 gel in wider glass vessels; they underwent phase separation.[24] A strain sweep at 1.0 rad/s on a 2.1 wt % **HSN-3**/CCl_4 gel at 15 °C indicated a yield strain limit of 0.01% (Supporting Information Figure S21).

The rheological experiments were difficult and limited in scope because liquid evaporated from the samples with time, especially near the edges of the rheometer plates (i.e., at the interface between the gel and air). Saturating the rheometer chamber with CCl_4 slowed the loss of liquid but did not stop it. Thus, measurements on samples had to be conducted rapidly, especially above room temperature. Figure 5A shows that storage modulus (G') and loss modulus (G'') are independent of the applied frequency at 15 °C in the linear viscoelastic regime. Figure 5B plots the moduli of a 1.9 wt % **HSN-3**/CCl_4 gel at a sequence of temperatures within the opaque (15 °C twice), clear (45 °C twice; the phase transition occurs at 37 °C), and opaque (15 °C twice) phases at a frequency of 100 rad/s. The most important observation from these data is that G' remains higher than G'' in both the lower- and higher-temperature gel phases: at 15 °C, G' and G'' were ∼4600 and ∼900 Pa, respectively; at 45 °C, they were ∼800 and ∼80 Pa. Because the data are obtained at one frequency only (for reasons given above), it is not possible to state definitively that these sample are gels at 45 °C.

Structures of Gel Networks. The network structures for the CCl_4 gels appear to be fibrillar in nature. In some gels, especially those at higher temperatures, their networks consisted of units too small to be detected by optical microscopy. In others, spherulitic objects were present (see Supporting Information Figures S16, S22−S25). A discussion of the structures of the SAFINs for the gels at different length scales will be presented individually for **HSN-*n*** (where n = 1, 3, 4, and 5). Although the most extensive investigation has been conducted with gels of **HSN-3**, sufficient information is available for the other gels to make interesting conclusions and to identify differences. In the absence of polarizers, for **HSN-4**/CCl_4 gel, fibrous networks are not clearly visible by optical microscopy, but they are visible in the **HSN-2**/CCl_4 and **HSN-3**/CCl_4 gels. With crossed-polars, the spherulites in all three gels are easily seen, but those of **HSN-4** are much smaller than those of **HSN-2** and **HSN-3** (Supporting Information Figures S16 and S23).

*Gels of 18-(Propylamino)octadecan-7-ol (**HSN-3**).* At 1 wt % and higher, **HSN-3**/CCl_4 gels are opaque. The POM of a transparent 0.5 wt % **HSN-3**/CCl_4 gel also shows a fiber-like texture (Supporting Information Figure S25). Unfortunately, this gel is too dilute for an XRD analysis to be performed. The optical micrograph of a 1.0 wt % **HSN-3**/CCl_4 gel at room temperature (i.e., the lower-temperature gel phase) reveals a spherulitic pattern (Figure 6A). Diffractograms of a 5.2 wt % **HSN-3**/CCl_4 gel were obtained at 22 and 55 °C (i.e., below and above T_{gg}) and compared with the diffraction pattern from neat **HSN-3** prepared by precipitation from a mixture of 1:4 (v:v) ethyl acetate:hexane (Figure 7). Although the signal-to-noise ratios of the diffraction patterns from the two gel phases are not good, it is clear that they are different from each other and from that of neat **HSN-3**. Attempts to index the diffraction peaks

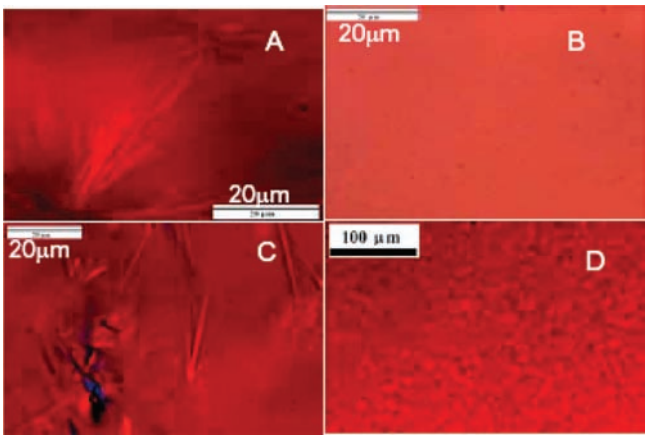

Figure 6. Polarizing optical micrographs (taken with a full-wave plate) of a 1.0 wt % **HSN-3**/CCl_4 gel (A) at 24 °C and (B) at 35 °C prepared by incubating the sol at 0 °C, (C) at 24 °C prepared by incubating the sol at 10 °C, and (D) at 24 °C prepared by incubating the sol at 20 °C.

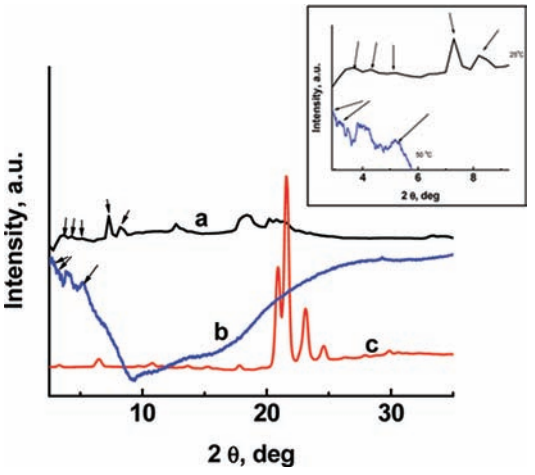

Figure 7. Vertically offset XRD patterns of a 5.2 wt % **HSN-3**/CCl_4 gel after empirical subtraction of the solvent diffraction at (a) 22 and (b) 55 °C and (c) of the diffraction of neat **HSN-3**. The inset shows the expanded 1−10° regions of (a) and (b).

according to their Bragg distances (Supporting Information Table S8)[22] and, thereby, to identify the gross natures of their cell packing were unsuccessful. Part of the problem may be the coexistence of two crystal morphs in the opaque gel phase. Although an insufficient number of peaks is discernible in the transparent gel phase for indexing, the network appears to be less crystalline than the lower-temperature phase (based upon the lack of diffraction peaks in the 15−25° regions), and the longest lattice spacing is near the calculated extended length of a molecule of **HSN-3**.

The IR spectra of both a 0.2 wt % **HSN-3**/CCl_4 sol/solution and a 1.1 wt % **HSN-3**/CCl_4 gel at 24 °C exhibit an OH-stretching at 3630 cm^{-1} (Figure 8) which is not observed for neat **HSN-3** (see Figure 1II, c) and which appears to be from an OH stretch that is not involved in hydrogen-bonding interactions. Similar absorption bands, reported for other alcohols in CCl_4 and other solvents,[25] have been assigned to the stretching of OH groups not involved in hydrogen-bonding interactions.[26] Note that 0.4 wt % (i.e., the CGC) of the 1.1 wt % **HSN-3** in the Figure 8a sample remains dissolved and not a part of the SAFIN.

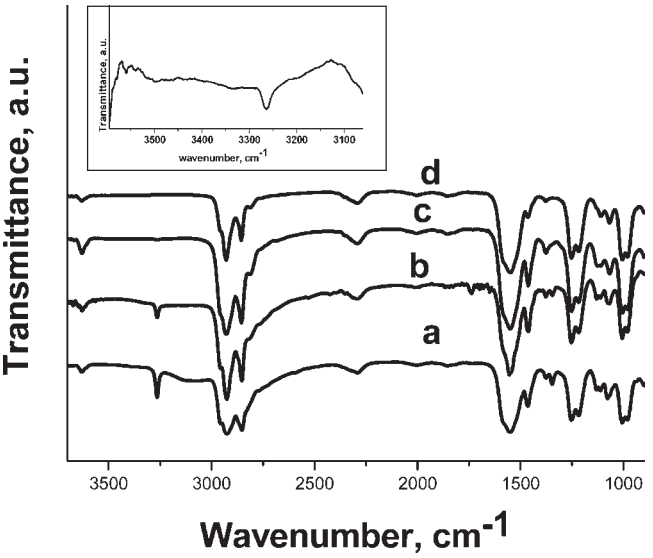

Figure 8. IR spectra of different concentrations of **HSN-3** in CCl_4 (sol/solution and gel) at 24 °C: (a) 1.1 wt % gel, (b) 0.6 wt % gel, (c) 0.4 wt % gel, and (d) 0.2 wt % sol/solution. The inset is an expansion of the 3000−3600 cm^{-1} region in spectrum (c), to show the weakness or absence of OH- and NH-stretching peaks.

Another striking feature of the spectra in Figure 8 is the absence of the NH-stretching peak at 3270 cm^{-1} in the sol/solutions. At the CGC of **HSN-3**, 0.4 wt %, the NH-stretching frequency is observed at 3270 cm^{-1} (see inset of Figure 8), and its intensity increases with increasing concentration. In solutions of dipropyl amine in CCl_4, the NH-stretching band has been shown to become progressively broader as concentration is lowered as a result of rapid exchange between "free" and hydrogen-bonded NH populations.[27] A similar phenomenon appears to be occurring here, and the 3270 cm^{-1} peak is attributed to NH that is involved in hydrogen-bonding interactions with OH (such as those indicated in the single-crystal structure of **HSN-3**; Figure 1I). The ratios of the peak areas between the OH (from 3670 −3550 cm^{-1}) or NH (from 3300 to 3220 cm^{-1}) stretch and the methylene stretches (3050−2575 cm^{-1}), an indicator of the relative populations of the free and hydrogen-bonded (NH−OH) OH environments, demonstrate that the latter are associated primarily with the SAFIN-incorporated molecules of **HSN-3** (Supporting Information Figure S26).

The IR spectrum of the 1.1 wt % **HSN-3**/CCl_4 gel in its clear phase, at 51 °C, lacks detectable NH peaks (3270 cm^{-1}) and OH peaks (3120 cm^{-1}) that involve hydrogen-bonding interactions (Figure 9a). Although the gel is still present and, therefore, a SAFIN must be present, hydrogen-bonding interactions must be severely weakened. Consistent with the visual and DSC observations reported above, the temperature-induced spectral changes are reversible: cooling the 1.1 wt % **HSN-3**/CCl_4 gel from 51 to 25 °C results in an IR spectrum very similar to that recorded before heating—hydrogen-bonded NH and OH peaks reappear (Figure 9). The ratios of the area of the OH (3670 −3550 cm^{-1}) or NH peak (3300−3220 cm^{-1}) and that of the methylene peak (3050−2575 cm^{-1}) at 25 °C before and after heating are 0.04 and 0.08, respectively, while those at 51 °C are 0.11 and 0.0.

In order to probe the structural rearrangements accompanying the gel-to-gel transition, SANS and USANS studies were carried out on gels containing 0.5, 1.0, and 2.0 wt % of **HSN-3**/CCl_4

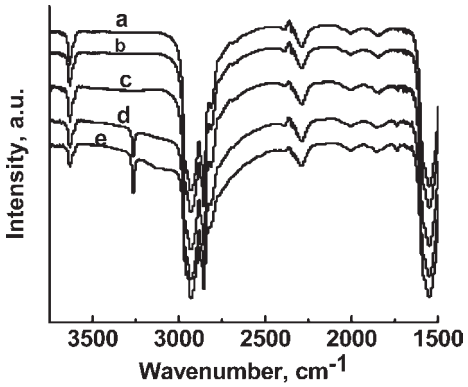

Figure 9. IR spectra of a 1 wt % 18-(propylamino)octadecan-7-ol (**HSN-3**) in CCl_4 gel at different temperatures recorded in the sequence indicated: (a) 51 °C, (b) 32 °C, (c) 25 °C after 10 min, (d) 25 °C after 1 h, and (e) 25 °C after 2 h.

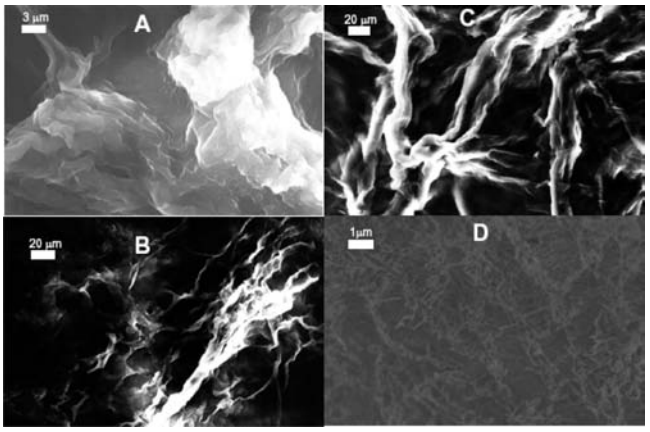

Figure 10. SEM images of xerogels prepared from (A) 0.5, (B) 1.0, and (C) 2.0 wt % **HSN-3**/CCl_4 gels. (D) A cryo-SEM image of a 1.1 wt % **HSN-3**/CCl_4 gel.

(Supporting Information Figure S27). Because the SANS scattering curves at 25 (opaque gel) and 50 °C (clear gel) are nearly identical, only minor differences must be present in the two SAFINs at distance ranges from 1 nm to several micrometers; the local fibril structure is not affected perceptibly by the opaque-to-clear gel phase transition. We anticipated, incorrectly, that the gel-to-gel transition would be related to large-scale structural changes within this distance regime.

The low-Q scattering follows a power law that eventually approaches a -1.5 slope in all cases at the lowest Q of 0.0001 $Å^{-1}$ (micrometer regime). For the 2.0 wt % **HSN-3**/CCl_4 gel at $Q >$ 0.015 $Å^{-1}$, the SANS curves at 25 and 50 °C are essentially identical, suggesting that the local structure, on length scales between 1 and 100 nm, such as the fibrils themselves, remains unchanged. However, scattering intensities for this gel at $Q <$ 0.015 $Å^{-1}$ differ slightly, with the intensity from the clear gel being about 20% lower than that of the opaque gel at Q = 0.001 $Å^{-1}$. Lower scattering intensities are also evident for the clear gels in the even lower Q regions examined by USANS (Supporting Information Figure S28). Lower intensities at higher temperatures would be a logical consequence of more of the LMOG being dissolved in higher-temperature CCl_4. However, such material loss cannot, in this case, come from the fibrillar network gel. Indeed, loss of LMOG from the fibrillar network would scale the entire curve down by a simple factor. Only LMOG bound in dense, large (micrometer size) structures, which do not participate in the higher Q scattering, could potentially, upon dissolution, lead to the different degree of intensity changes observed at different Q values. Similarly, the slight intensity decrease at low Q cannot be due to simply a contrast change (which could originate, for example, from a density change in either the solvent or the fibers, including solvent moving in to or out of individual fibers).

Possible interpretations include (1) the formation at high temperatures of very large scale heterogeneities (nearly millimeter length scales), (2) the lowering of density of the gel network or the size of the inhomogeneities in that network, and (3) the melting of small (micrometer size) crystallites. The first is difficult to accept unless the objects are perfectly index-matched to the matrix in which they form. The second interpretation could arise, for example, if the fibrils become significantly more flexible in the higher-temperature phase, or if solvent content in the fibril-rich regions changes (i.e., those regions become more or less dense). For a fixed total volume, the average "mesh size" would be expected to increase, leading to a more open gel network. Without a loss or gain of material contributing to the scattering, any lowered intensity would need to be compensated for by an increased intensity at another Q, which does not seem to be the case. Given the very small decrease at very low Q and the fact that the area under the curve times Q is (IQ^2) invariant, it is conceivable that the required change at higher Q is hidden within the experimental uncertainty. This leads directly to the third interpretation: below T_{gg}, two different morphs coexist, and they melt at different temperatures. In this case, the increased intensity at low Q and low temperatures would originate from that very small amount of extra material in the large length scale regime. The crystallites could melt to become molecularly dispersed or simply become small chunks of rod-like objects, similar in diameter to the fibrils of the other morph without contributing significantly to the scattered signal. However, two observations—that some homologues of the **HSN-*n*** which remain transparent throughout the heating and cooling cycles also show first-order transitions by DSC and that the lower- and higher-temperature gel phases have different packing patterns, as indicated by the XRD data in Figure 7—make this interpretation unlikely. On these bases, we favor the second interpretation that attributes the SANS results to the lowering of either the density of the gel network or the size of the inhomogeneities in that network as a result of loss of solvent molecules between fibers in bundles.

Finally, because the scattering is directly proportional to concentration, subtracting the solvent background contribution from each data set and then normalizing the curves to concentration, as done in Supporting Information Figure S29, helps to highlight the structural changes alone. Interestingly, the two concentrations that are in the concentration regime where the gel-to-gel transitions are observed (i.e., 1.0 and 2.0 wt %) have very similar local structural signatures, with a cross-sectional diameter of the gel fibers of ~30 nm, while the lower concentration (that exhibits only a gel-to-sol transition) has a markedly smaller fibril diameter, ~15 nm. These diameters are obtained by both a modified Guinier fit and a flexible cylinder form factor fit, with the range of the fit restricted to $Q >$ 0.015 or 0.02 $Å^{-1}$, depending on the curve. Thus, it appears that the gel-to-gel transition may only occur once the fibrils reach a 30 nm diameter,

and bundling/unbundling phenomena of the fibers may be implicated in the changes.[28]

Figure 6A,C,D shows the influence of the protocol for cooling a sol on the eventual fibrillar structure of the gels. The textures of the gels from incubation at 10 and 20 °C (i.e., near the T_{gg}, 27−32 °C) are very different. Although the gel from incubation at 20 °C was transparent to the eye, a pattern of very small objects could be detected with the aid of light polarizers.

By SEM (Figure 10), the xerogels from a transparent (0.5 wt %) gel of **HSN-3** in CCl_4 showed plate-like structures, whereas twisted fibrous bundles, with a pitch ∼5 μm, are present in the xerogels from the opaque (1.0 and 2.0 wt %) gels. As suggested above, bundling probably occurs as the CCl_4 evaporates and the concentration of fibrous objects increases. Because removal of the liquid can cause even more drastic morphological changes, a cryo-SEM image of a 1.1 wt % **HSN-3**/CCl_4 gel (Figure 10D) was also obtained. It shows fibers having ∼60 nm diameters (average for 10 fibers) as well as plate-like structures, but smaller than those found in the SEM images. The selection of images at different magnifications in Supporting Information Figure S30 is representative of the structures found. The sum of the observations from these images supports our hypothesis that two kinds of morphs coexist in the gels of **HSN-3** in CCl_4.

*Gels of 18-(Butylamino)octadecan-7-ol (**HSN-4**).* The diffractograms of a xerogel prepared by drying a 5 wt % **HSN-4**/CCl_4 gel (Supporting Information Figure S31) and of the neat solid (crystallized from 1:4 (v:v) ethyl acetate:hexane) are the same, but the diffractogram of the gel itself at 22 °C consists of a broad and almost featureless pattern. The gel pattern at 58 °C consists of sharp reflections from a very different morph than the one in the xerogel or neat solid. The fact that the diffraction patterns from neat solid after removal of CCl_4 and from the gel at 58 °C are different eliminates the possibility that some crystallized **HSN-4** as a (bulk) phase-separated material is responsible for the gel diffraction. These observations suggest that the SAFIN is less crystalline in the lower-temperature gel phase. In addition, the X-ray diffractograms recorded at 22 °C starting 7 h and 2 weeks after heating to 58 °C showed that the SAFIN of the gel phase at 58 °C returns very slowly to the "equilibrated" lower-temperature phase.

Although the IR spectra of neat solids **HSN-3** and **HSN-4** are similar, the IR spectra of their gels are not (Supporting Information Figure S32). The spectrum of a 1.0 wt % **HSN-4**/CCl_4 gel at 24 °C lacks a sharp NH-stretching peak (3270 cm^{-1}) and a broader and weak free OH-stretching peak (3630 cm^{-1}) that is found in the spectrum of the corresponding gel of **HSN-3**; packing within the two SAFINs must differ near these groups. At 50 °C, the "free OH-stretching" peak at 3630 cm^{-1} of the **HSN-4**/CCl_4 gel became sharper and was almost unchanged 3 h after the gel was returned to 25 °C.

This observation is consistent with the hysteresis noted above in the DSC thermograms and X-ray diffractograms of **HSN-4**/CCl_4 gels. One hypothesis for these observations is that CCl_4 molecules reside inside fibers or, more probably, between fibers in bundles of the lower-temperature SAFIN and are expelled from them in the higher-temperature phase. Re-entry into the fibers or between them is slow because the packing arrangement of **HSN-4** must adapt to the changes required to accommodate the liquid molecules. Examples of other organogels with SAFINs that include some liquid component are known.[29] Perhaps the most well studied case of solvent expulsion at higher temperatures involves the somewhat related clear-to-opaque lower critical solution temperature transition that occurs when hydrogels of poly(isopropyl acrylamide) are warmed.[11]

Scheme 1. Cartoon Representation of (Top) Possible Temperature-Induced Structural Changes Occurring during Gel-to-Gel Transitions within a Two-Dimensional Slice of a Fiber, Where Red and Blue Circles Indicate OH and NH Groups, and (Bottom) Loss of CCl_4 Molecules (Green Circles) from between Fibers within Bundles in the Networks of HSN-*n*/CCl_4 Gels

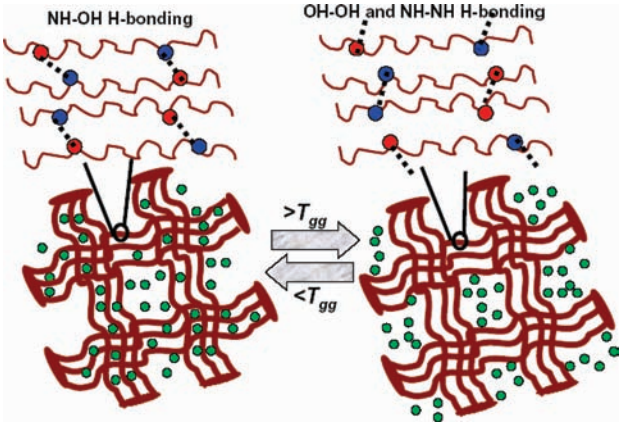

*Gels of 18-(Methylamino)octadecan-7-ol (**HSN-1**) and 18-(Pentylamino)octadecan-7-ol (**HSN-5**).* "Amorphous-like" diffractograms were also found for gels of **HSN-1**/CCl_4 and **HSN-5**/CCl_4 at room temperature (Supporting Information Figure S33), like that of the lower-temperature gel of **HSN-4**/CCl_4, and the diffractograms of the neat solids of **HSN-1** and **HSN-5** are almost the same as that of the neat solid of **HSN-4**. However, the **HSN-1**/CCl_4 and **HSN-5**/CCl_4 gels display none of the hysteresis or gel-to-gel phase transitions of the system with **HSN-4**. IR spectra of 1 wt % **HSN-1**/CCl_4 and **HSN-5**/CCl_4 gels at 25 °C show peaks at 3630 cm^{-1} from free OH-stretching as well as broad peaks centered around 3375 and 3213 cm^{-1} (Supporting Information Figure S34). As mentioned, the IR spectrum of dipropylamine in CCl_4 contains two broad peaks centered at ∼3328 and ∼3289 cm^{-1}.[27] At 50 °C, the peaks centered at 3375 cm^{-1} become much weaker. One possible reason for the absence or broadening of the NH-stretching peak (expected at 3270 cm^{-1} on the basis of the crystal structure of **HSN-5**; see Figure 1) in the IR spectra of the **HSN-1** and **HSN-5** gels may be weakened NH−OH hydrogen-bonding interactions. In this case, the ∼3375 and ∼3213 cm^{-1} peaks can be assigned to free and hydrogen-bonded NH-stretching vibrations, respectively.

CONCLUSIONS

The sources of the unprecedented thermally reversible, gel-to-gel transformations of CCl_4 gels with some low-molecular-mass organogelators, (*R*)-18-(*n*-alkylamino)octadecan-7-ols, have been identified. The closest analogy we can find with these systems is the heating transition of *hydro*gels of a *polymeric* gellant, poly(*N*-isopropyl acrylamide), in which water molecules are expelled from the network, causing a *conformational* change of the polymer chains to more globular than their lower-temperature extended forms.[11] The differences are even more fundamental: in the hydrogel, the loss of water initiates the change of

the polymer shape; in the **HSN-*n***/CCl_4 systems, changes in the molecular packing arrangements within the gelator fibers initiate the loss of the liquid. It is surprising that the transformations in the organogel systems examined here are limited to CCl_4, although similar changes were sought with a wide range of liquids. We conjecture that both polarity and molecular size and shape contribute to the uniqueness of CCl_4 here. A cartoon representation of the structural changes thought to be occurring in the transformations is shown in Scheme 1. In the lower-temperature gel phase, CCl_4 molecules are able to reside between (and perhaps within) fibers of bundles that constitute the fibrillar networks. At the heating transition, a first-order process, the changes in hydrogen-bonding arrangements that attend the modification of the molecular packing arrangement within the fibers force the expulsion of some (or all) of the CCl_4 molecules. Cooling the higher-temperature gel phase allows the original molecular packing arrangement to be reformed and the CCl_4 molecules to re-enter the fibrillar network.

In some cases, the re-entry of the liquid is very fast; in others, it is not and there is significant hysteresis. The times required for the liquid to re-enter appear to be related to the specific differences between the lower- and higher-temperature packing arrangements in the **HSN-*n*** morphs. Thus, there was no detectable hysteresis upon cooling the clear **HSN-3**/CCl_4 gel to its opaque form; re-entry of expelled CCl_4 molecules into the SAFIN is rapid. By contrast, considerable hysteresis was found when the higher-temperature form of the **HSN-4**/CCl_4 gel was cooled. These differences must be related to the specific packing arrangements of the **HSN-*n*** molecules within their lower- and higher-temperature fibers. At this point, we lack the detailed information necessary to make definitive statements about how one methylene group—the difference between the structures of **HSN-3** and **HSN-4**—can be responsible for the kinetic differences observed in the gel-to-gel transitions *or* why other homologues do not undergo a gel-to-gel transition. In addition to the obvious packing differences that longer and shorter *N*-alkyl chains can cause, the dependence of *trans*−*gauche* conformational changes on the length of the *N*-alkyl chains may also be important,[30] and we will attempt to investigate them in the future by introducing *E*- and *Z*-alkenyl groups in place of the saturated alkyl substituents.

This study offers opportunities to design new gelators that are capable of behaving in multiple fashions without entering the sol/solution phase, and it identifies a heretofore unknown transformation of organogels.

■ ASSOCIATED CONTENT

Ⓢ Supporting Information. Crystal data and refinement for **HSN-5** (also as a CIF file); crystal packing information, XRD diffractograms, DSC thermograms, and melting temperatures of neat **HSN-*n***; DSC thermograms of **HSN-*n*** (n = 1, 4, and 5)/CCl_4 gels; POMs of **HSN-*n***/CCl_4 gels at different temperatures; plots of T_{gs} versus concentration for **HSN-1**/CCl_4 and **HSN-4**/CCl_4 gels; plots of relative turbidity (scattering intensities) versus temperature from **HSN-3**/CCl_4 and **HSN-4**/CCl_4 gels; heats of transition for different concentrations of **HSN-3**/CCl_4 gels; Schröder−van Laar plots and calculated enthalpies of **HSN-3**/CCl_4 gels; strain sweep plot of a **HSN-3**/CCl_4 gel; SANS/USANS intensity versus Q plots for **HSN-3**/CCl_4 gels at different concentrations above and below T_{gg}; and IR spectra of **HSN-*n*** (n = 1, 4, and 5)/CCl_4 gels at different temperatures. This material is available free of charge via the Internet at http://pubs.acs.org.

■ AUTHOR INFORMATION

Corresponding Author
weissr@georgetown.edu

■ ACKNOWLEDGMENT

The National Science Foundation is thanked for its support of this research. We are grateful to Dr. Jibao He and Prof. Vijay John of Tulane University for recording the cryo-SEM images and to Prof. Daniel Blair of the Georgetown Physics Department for the use of his rheometer. This work utilized facilities supported in part by the National Science Foundation under Agreement No. DMR-0944772. We acknowledge the support of the National Institute of Standards and Technology, U.S. Department of Commerce, in providing the neutron research facilities used in this work.

■ REFERENCES

(1) (a) Terech, P.; Weiss, R. G. *Chem. Rev.* **1997**, *97*, 3133–3159. (b) Shinkai, S.; Murata, K. *J. Mater. Chem.* **1998**, *8*, 485–495. (c) Abdallah, D. J.; Weiss, R. G. *Adv. Mater.* **2000**, *12*, 1237–1247. (d) van Esch, J. H.; Feringa, B. L. *Angew. Chem., Int. Ed.* **2000**, *39*, 2263–2266. (e) Sangeetha, N. M.; Maitra, U. *Chem. Soc. Rev.* **2005**, *34*, 821–836. (f) Weiss, R. G., Terech, P., Eds. *Molecular Gels. Materials with Self-Assembled Fibrillar Networks*; Springer: Dordrecht, 2006. (g) George, M.; Weiss, R. G. *Acc. Chem. Res.* **2006**, *39*, 489–497.

(2) van Esch, J. H.; Schoonbeek, F.; Loos, M. D.; Veen, E. M.; Kellog, R. M.; Feringa, B. L. In *Supramolecular Science: Where It Is and Where It Is Going*; Ungar, R., Dalcanale, E., Eds.; Kluwer Academic Publishers: The Netherlands, 1999; pp 233−259.

(3) (a) Dastidar, P. *Chem. Soc. Rev.* **2008**, *37*, 2699–2715. (b) Liu, X. Y. *Top. Curr. Chem.* **2005**, *256*, 1–37.

(4) Li, Y.; Tanaka, T. *Annu. Rev. Mater. Sci.* **1992**, *22*, 243–277.

(5) Kato, T.; Hirai, Y.; Nakaso, S.; Moriyama, M. *Chem. Soc. Rev.* **2007**, *36*, 1857–1867.

(6) Kotlewski, A.; Norder, B.; Jager, W. F.; Picken, S. J.; Mendes, E. *Soft Matter* **2009**, *5*, 4905–4913.

(7) (a) Yagai, S.; Ishii, M.; Karatsu, T.; Kitamura, A. *Angew. Chem., Int. Ed.* **2007**, *46*, 8005–8009. (b) Zhu, G. Y.; Dordick, G. S *Chem. Mater.* **2006**, *18*, 5988–5995. (c) Wang, R. Y.; Liu, X. Y.; Xiong, J. Y.; Li, J. L. *J. Phys. Chem. B* **2006**, *110*, 7275–7280. (d) Tung, S. H.; Huang, Y. E.; Raghavan, S. R. *Soft Matter* **2008**, *4*, 1086–1093.

(8) (a) Zhu, P. L.; Yan, X. H.; Su, Y.; Yang, Y.; Li, J. B. *Chem. Eur. J.* **2010**, *16*, 3176–3183. (b) Cui, J. X.; Shen, Z. H.; Wan, X. H. *Langmuir* **2010**, *26*, 97–103. (c) Kuang, G.-C.; Teng, M.-J.; Jia, X.-R.; Chen, E.-Q.; Wei, Y. *Chem. Asian J.* **2011**, *6*, 1163–1170.

(9) (a) Lin, Y.; Kachar, B.; Weiss, R. G. *J. Am. Chem. Soc.* **1989**, *111*, 5542–5551. (b) Furman, I.; Weiss, R. G. *Langmuir* **1993**, *9*, 2084–2088. (c) Rogers, M. A.; Marangoni, A. G. *Cryst. Growth Des.* **2008**, *8*, 4596–4601. (d) Huang, X.; Terech, P.; Raghavan, S. R.; Weiss, R. G. *J. Am. Chem. Soc.* **2005**, *127*, 4336–4344. (e) Huang, X.; Terech, P.; Raghavan, S. R.; Weiss, R. G. *J. Am. Chem. Soc.* **2006**, *128*, 15341–15352.

(10) Mallia, V. A.; George, M.; Blair, D. L.; Weiss, R. G. *Langmuir* **2009**, *25*, 8615–8625.

(11) (a) Schild, H. G. *Prog. Polym. Sci.* **1992**, *17*, 163–249. (b) Hirokawa, Y.; Tanaka, T. *J. Chem. Phys.* **1984**, *81*, 6379–6380.

(12) (a) Zhang, X.-Z.; Xu, X.-D.; Cheng, S.-X.; Zhuo, R.-X. *Soft Matter* **2008**, *4*, 385–391. (b) Qiu, Y.; Park, K. *Adv. Drug Delivery Rev.* **2001**, *53*, 321–339.

(13) Takahashi, A.; Sakai, M.; Kato, T. *Polym. J.* **1980**, *12*, 335–341.

(14) Sheldrick, G. M. *Acta Cryst.* **2008**, A64, 112−122.

(15) Barbour, L. J. *J. Supramol. Chem.* **2001**, *1*, 189–191.
(16) Glinka, C.; Barker, J.; Hammouda, B.; Krueger, S.; Moyer, J.; Orts, W. *J. Appl. Crystallogr.* **1998**, *31*, 430–445.
(17) Kline, S. R. *J. Appl. Crystallogr.* **2006**, *39*, 895–900.
(18) Barker, J. G.; Glinka, C.; Moyer, J. J.; Kim, M. H.; Drews, A. R.; Agamalian, M. *J. Appl. Crystallogr.* **2005**, *38*, 1004–1011.
(19) (a) Terech, P.; Rodriguez, V.; Barnes, J. D.; Mckenna, G. B. *Langmuir* **1994**, *10*, 3406–3418. (b) Terech, P.; Pasquier, D.; Bordas, V.; Rossat, C. *Langmuir* **2000**, *16*, 4485–4494. (c) Tsau, J. S.; Heller, J. P.; Pratap, G. *Polym. Prepr.* **1994**, *35*, 737–738. (d) Tachibana, T.; Mori, T.; Hori, K. *Bull. Chem. Soc. Jpn.* **1980**, *53*, 1714–1719. (e) Tachibana, T.; Mori, T.; Hori, K. *Bull. Chem. Soc. Jpn.* **1981**, *54*, 73–80. (f) Tachibana, T.; Kitazawa, S.; Takeno, H. *Bull. Chem. Soc. Jpn.* **1970**, *43*, 2418–2421. (g) Tachibana, T.; Kambara, H. *Bull. Chem. Soc. Jpn.* **1969**, *42*, 3422–3424. (h) Tachibana, T.; Kambara, H. *J. Am. Chem. Soc.* **1965**, *87*, 3015–3016. (i) Terech, P. *Colloid Polym. Sci.* **1991**, *269*, 490–500.
(20) Cole, E. A.; Holmes, D. R. *J. Polym. Sci., Part A* **1960**, *46*, 245–246.
(21) Iwasaki, A.; Fujii, A.; Watanabe, T.; Ebata, T.; Mikami, N. *J. Phys. Chem.* **1996**, *100*, 16053–16057.
(22) It should be noted that, although indexing of X-ray reflections here and in other samples was performed using all detectable peaks, the true packing arrangement may be different from that determined by the Jade software because the number of reflection peaks is relatively small and the signal-to-noise ratios of some diffractograms are low.
(23) For the same reasons, plots of the mole fraction of the **HSN-3**/CCl_4 gels versus T_m^{-1} according to the Schröder−van Laar equation[23a,b] (Supporting Information Figures S18 and S19 and Table S5) fail to yield reasonable heats for the gel-to-gel transition. This type of data treatment is valid only when two conditions are met: (1) the gels melt to an ideal solution and (2) the concentration of gelator within the fibrillar networks is equal to the bulk concentration minus the CGC. Although our data treatment can correct for the second condition, it cannot for the first. (a) Atkins, P. W. *Physical Chemistry*, 5th ed.; Freeman: New York, 1994; p 227. (b) Moore, W. J. *Physical Chemistry*, 4th ed.; Prentice Hall: Englewood, Cliffs, NJ, 1972; p 249.
(24) Raghavan, S. R.; Cipriano, B. H. In *Molecular Gels. Materials with Self-Assembled Fibrillar Networks*; Weiss, R. G., Terech, P., Eds.; Springer: Dordrecht, 2006; pp 241−252.
(25) Symons, M. C. R.; Thomas, V. K. *J. Chem. Soc., Faraday Trans. 1* **1981**, *77*, 1883–1890.
(26) Kristiansson, O. *J. Mol. Struct.* **1999**, *477*, 105–111.
(27) Rocher, N.; Roger Frech, R. *J. Phys. Chem. A* **2007**, *111*, 2662–2669.
(28) Pashuck, E. T.; Cui, H.; Stupp, S. I. *J. Am. Chem. Soc.* **2010**, *132*, 6041–6046.
(29) See, for example: (a) Wang, R.; Geiger, C.; Chen, L.-H.; Swanson, B.; Whitten, D. G. *J. Am. Chem. Soc.* **2000**, *122*, 2399–2400. (b) Duncan, D. C.; Whitten, D. G. *Langmuir* **2000**, *16*, 6445–6452.
(30) Vaia, R. A.; Teukolsky, R. K.; Giannelis, E. P. *Chem. Mater.* **1994**, *6*, 1017–1022.